Nonisothermal Crystallization Kinetics of Poly(vinylidene fluoride) in a Poly(vinylidene fluoride)/Dibutyl Phthalate/Di(2-ethylhexyl)phthalate System via Thermally Induced Phase Separation

Gen-Liang Ji, Bao-Ku Zhu, Chun-Fang Zhang, You-Yi Xu

Department of Polymer Science and Engineering, Zhejiang University, Hangzhou 310027, China

Received 22 December 2006; accepted 29 August 2007
DOI 10.1002/app.27250
Published online 1 November 2007 in Wiley InterScience (www.interscience.wiley.com).

ABSTRACT: The nonisothermal crystallization kinetics of poly(vinylidene fluoride) (PVDF) in PVDF/dibutyl phthalate (DBP)/di(2-ethylhexyl)phthalate (DEHP) blends via thermally induced phase separation were investigated through differential scanning calorimetry measurements. The Ozawa approach failed to describe the crystallization behavior of PVDF in PVDF/DBP/DEHP blends, whereas the modified Avrami equation successfully described the nonisothermal crystallization process of PVDF. Two stages of crystallization were observed in this analysis, including primary crystallization and secondary crystallization. The influence of the cooling rate and DBP ratio in the diluent mixture on the crystallization mechanism and crystal structure was determined by this method. The Mo approach well explained the kinetics of primary crystallization. An analysis of these two methods indicated that the increase in the DBP ratio in the diluent mixture caused a decrease in the crystallization rate at the primary crystallization stage. The activation energy was determined according to the Kissinger method and also decreased with the DBP ratio in the diluent mixture increasing. © 2007 Wiley Periodicals, Inc. J Appl Polym Sci 107: 2109–2117, 2008

Key words: compatibility; crystallization; differential scanning calorimetry (DSC); kinetics (polym.); membranes

INTRODUCTION

In recent years, poly(vinylidene fluoride) (PVDF) has become a favorable choice as the polymer matrix for gel polymer electrolytes because of its appealing properties, such as a high dielectric constant (8.4) and strongly electron-withdrawing functional groups (—C—F). Generally, two methods for preparing PVDF gel electrolytes are employed. The most common approach is solvent casting.[1,2] According to this method, a mixture of PVDF, a lithium salt, and a plasticizer is formed in a glovebox and cast to form a gel electrolyte. On the other hand, the phase-inversion technique, suggested by Gozdz and coworkers,[3,4] is also a popular method for preparing PVDF gel electrolytes.[5–8] Compared with the solvent-casting technique, this method involves an activation process in which a PVDF membrane is soaked in an electrolyte solution and requires critical moisture control only at the time of assembling the cells. In the activation process of the phase-inversion technique, the liquid electrolyte is trapped in the porosity of the PVDF membrane but also swells the amorphous phase of PVDF. The PVDF crystalline phase is retained during the activation process and acts as a mechanical support for the PVDF gel electrolyte. The amorphous phase of PVDF helps to entrap a large amount of liquid electrolyte and contributes to preventing the leakage of the electrolyte. It seems that the crystallinity of the PVDF membrane becomes a double-edged sword for the ionic conductivity and mechanical strength of the PVDF gel electrolyte.

In the phase-inversion technique, highly porous PVDF membranes have been extensively prepared by Bellcore's technology (air casting of a polymer solution),[3–5] modifications of Bellcore's technology,[6,7] and immersion precipitation.[8] Recently, a few studies have been reported on the preparation of PVDF microporous membranes via thermally induced phase separation (TIPS).[9–11] TIPS has outstanding merits[12] and presents an alternate method for preparing porous PVDF membranes in the fabrication of gel polymer electrolytes. The TIPS process begins by the dissolution of a polymer in a diluent at an elevated temperature. The solution is then cast or extruded into the desired shape (flat sheet, hollow

Correspondence to: Y.-Y. Xu (opl-yyxu@zju.edu.cn).
Contract grant sponsor: National Basic Research Program of China; contract grant number: 2003CB615705.
Contract grant sponsor: National Nature Science Foundation; contract grant number: 50433010.

fiber, etc.) and cooled to induce phase separation and polymer solidification (crystallization or glass transition).[12,13] The diluent is extracted by solvent exchange, and the extractant is usually evaporated to yield a microporous structure. When thermal energy is removed from the homogeneous polymer–diluent mixture, TIPS can occur via solid–liquid (S–L) or liquid–liquid phase separation, depending on the polymer–diluent interaction, the composition, and the thermal diving force. In the process of TIPS, the crystallization of the polymer usually passes through a primary crystallization stage and a secondary crystallization stage.[14] Secondary crystallization as a source of structural evolution has been investigated in a variety of polymers, including ethylene/octane copolymers, poly(ether ether ketone), polycarbonate, and PVDF.[15–18] In these studies, secondary crystals forming in the secondary crystallization are described as small clusters of organized neighboring chain segments forming bundlelike or fringed-micellar structures with virtually no or few reentry foldings. Obviously, these secondary crystals contribute little to the mechanical strength of the gel polymer electrolyte. On the other hand, these secondary crystals make the swelling of the liquid electrolyte in the polymer more difficult.

The possible use of polymer nonisothermal crystallization in the TIPS process has been demonstrated only with S–L phase-separation TIPS.[19,20] The purpose of this work is to determine a proper nonisothermal crystallization model to describe the overall nonisothermal crystallization kinetics of PVDF in PVDF/dibutyl phthalate (DBP)/di(2-ethylhexyl)phthalate (DEHP) blends with only S–L phase separation during the TIPS process and to examine whether secondary crystallization of PVDF exists and how the diluent and cooling rate affect the kinetics of crystallization. The information gained from this study will be useful for determining the conditions of membrane fabrication via TIPS.

EXPERIMENTAL

Materials

The PVDF (number-average molecular weight = 59,000, weight-average molecular weight/number-average molecular weight = 2.88) used in the study was provided by Solvay Silexis (Brussels, Belgium) (1012) with a melt flow index of 1.5. DBP and DEHP, supplied by Guangdong Guanghua Chemical Factory Co., Ltd. (Guangdong, China), and Shanghai Chemical Reagent Co., Ltd. (Shanghai, China), respectively, were used for preparing the diluent mixture without further purification. Both DBP (bp = 340°C) and DEHP (bp = 386°C) have boiling points much higher than the melting point of PVDF (174°C) and dissolve in each other to become a homogeneous diluent mixture.

Preparation of the PVDF/DBP/DEHP blend samples

Diluent mixtures (DBP/DEHP) of known concentrations were prepared beforehand. Because PVDF hardly dissolves in pure DEHP at a higher temperature (240°C), diluent mixtures with the ratio of DBP to DEHP over 27.5 : 72.5 (w/w), in which PVDF dissolves more quickly to form a homogeneous solution at 240°C, were chosen as the latent diluents for this study. PVDF and the diluents were mixed at an elevated temperature (240°C) under a nitrogen atmosphere for at least 3 h in a glass vessel with a stirrer. Then, the glass vessel was quenched in liquid nitrogen to solidify the sample and broken open to obtain the solid polymer–diluent sample. Homogeneous samples of a 30 wt % PVDF blend with diluent mixtures of various DBP ratios were prepared; the details are given in Table I.

Observation of the phase separation

The type of phase separation for different systems was observed with optical microscopy. The prepared sample was heated slowly to 250°C and held at that temperature for 1 min to ensure complete dissolution. Subsequently, the sample was cooled to a required temperature at 10°C/min to give rise to phase separation. Four systems (S40, S50, S80, and S100), which had only S–L phase separation under observation, were chosen to study the nonisothermal crystallization behavior of PVDF in diluent mixtures.

Nonisothermal crystallization process

The nonisothermal crystallization behavior of PVDF in diluent mixtures was studied on a PerkinElmer (Waltham, MA) DSC-7. All differential scanning calorimetry (DSC) measurements were performed under a nitrogen atmosphere, and sample weights varied from 4 to 7 mg. To reveal the nonisothermal crystallization kinetics, the sample was first heated to 250°C and maintained at this temperature for 5 min to erase the thermal history, and then the sample was cooled at rates of 5, 10, 20, and 30°C/min to the final temperature of 40°C. The exothermic

TABLE I
Compositions of Various PVDF/DBP/DEHP Blends

Number	PVDF (wt %)	DBP/DEHP (w/w)
S40	30	40 : 60
S50	30	50 : 50
S80	30	80 : 20
S100	30	100 : 0

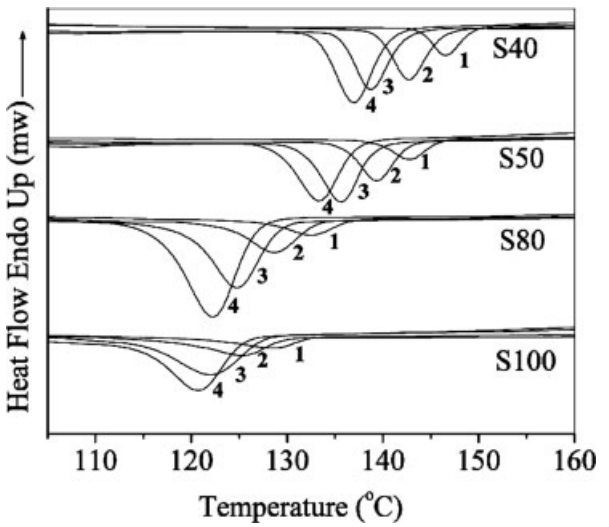

Figure 1 DSC curves of the nonisothermal crystallization of PVDF/DBP/DEHP blends at different cooling rates: (1) 5, (2) 10, (3) 20, and (4) 30°C/min.

curves of heat flow with different cooling rates were recorded and investigated.

RESULTS AND DISCUSSION

Nonisothermal crystallization

Figure 1 shows typical DSC curves of heat flow as a function of temperature at different cooling rates for different PVDF/DBP/DEHP blends.

In nonisothermal crystallization, the onset temperature of crystallization (T_o), the end temperature of crystallization (T_e), and the exothermic peak temperature of crystallization (T_p) were determined from curves, and the results are shown in Table II. All these parameters (T_o, T_e, and T_p) shifted to lower temperatures with the cooling rate increasing. This observation is typical and common for most semicrystalline polymers while crystallizing nonisothermally. When the polymer was undergoing crystallization at a lower cooling rate, it remained for a longer time within a specific temperature range to promote sufficient mobility of segments for the growth of crystallization. When it was cooled at a relatively rapid rate, however, segments were frozen before the formation of regular crystallization, and this reduced the crystallization temperature.

It was also evident that with an increasing DBP ratio in the diluent mixture, all the parameters likewise decreased. The overall feature in Table II is analyzed in terms of the interaction between PVDF and the diluent mixture and the viscosity of the system. The estimated interaction parameter (χ^*), typically used to interpret the interaction between the polymer and the diluent, was estimated from the difference of the solubility parameters between the polymer and the diluent with the following expression:[21]

$$\chi^* = \frac{V_m}{RT}[[\delta_{d1} - \delta_{d2}]^2 + [\delta_{p1} - \delta_{p2}]^2 + [\delta_{h1} - \delta_{h2}]^2]$$

where V_m is a reference volume that equals the molar volume of the specific repeating unit size of the polymer; δ_d and δ_p are the dispersive and polar terms of the solubility parameter, respectively; δ_h is the hydrogen-bonding contribution to the solubility parameter; 1 and 2 refer to the diluent and polymer, respectively; R is the ideal gas constant; and T is the absolute temperature. From the Hansen solubility parameters of PVDF, DBP, and DEHP summarized in Table III,[22] it was found that the differences in the Hansen solubility parameters ($\Delta\delta_d$, $\Delta\delta_p$, $\Delta\delta_h$, and $\Delta\delta$) between PVDF and DBP were much smaller than those between PVDF and DEHP, which showed that DBP had better interaction with PVDF than DEHP. As a result, the interaction between PVDF and the diluent mixture was enhanced by the DBP ratio increasing in the diluent mixture. On the other hand,

TABLE II
Nonisothermal Parameters for PVDF in PVDF/DBP/DEHP Blends Determined from DSC Exotherms

Cooling rate (°C/min)	Crystallization parameters (°C)	S40	S50	S80	S100
5	T_o	149.4	146.0	136.6	132.5
	T_e	141.5	134.0	119.6	115.4
	T_p	146.5	142.7	132.5	128.5
10	T_o	146.2	142.7	133.1	129.7
	T_e	137.1	132.3	115.9	110.2
	T_p	142.7	139.4	128.7	125.4
20	T_o	142.3	139.1	129.2	127.6
	T_e	130.7	128.2	113.0	108.2
	T_p	138.8	135.7	124.7	122.0
30	T_o	140.7	137.2	126.7	125.3
	T_e	128.8	124.8	110.5	107.6
	T_p	137.1	133.2	122.3	120.8

TABLE III
Hansen Solubility Parameters of PVDF, DBP, and DEHP at 25°C

Substance	δ_d [(MPa)$^{1/2}$]	δ_p [(MPa)$^{1/2}$]	δ_h [(MPa)$^{1/2}$]	δ [(MPa)$^{1/2}$]
DBP	17.8	8.6	4.1	20.3
DEHP	16.6	7.0	3.1	18.2
PVDF	17.2	12.5	9.2	23.2

DBP possesses a higher viscosity than DEHP [DBP, 163 mPa s (20°C), and DEHP, 80 mPa s (20°C)], so the viscosity of the system increased with the DBP ratio increasing. These two factors led to lower mobility of the polymer segments and prevented crystal nucleation and growth of PVDF as the DBP ratio increased. As a result, the system needed deeper supercooling to form the crystal nuclei of PVDF, and the crystallization temperature decreased as the DBP ratio increased.

The determination of the absolute crystallinity is not required for the analysis of crystallization kinetics, and the relative degree of crystallinity as a function of temperature [$X(T)$] is defined as follows:

$$X(T) = \frac{\int_{T_0}^{T}(dH_C/dT)dT}{\int_{T_0}^{T_\infty}(dH_C/dT)dT} \quad (1)$$

where T_0 and T_∞ are the onset and end crystallization temperatures, respectively, and dH_C/dT is the heat flow rate. In nonisothermal crystallization, time t is related to temperature T as follows:

$$t = \frac{T_0 - T}{\Phi} \quad (2)$$

where T is the temperature at time t, T_0 is the temperature at which the crystallization begins ($t = 0$), and Φ is the cooling rate. The development of the relative crystallinity with the time for PVDF/DBP/DEHP blends is shown in Figure 2.

The crystallization half-time ($t_{1/2}$) is defined as the time at which the relative crystallization degree is 50% completed. $t_{1/2}$ is usually used to present the overall crystallization rate. Figure 3 shows the dependence of $t_{1/2}$ on the DBP ratio in the diluent mixture and the cooling rate. $t_{1/2}$ increased as the DBP

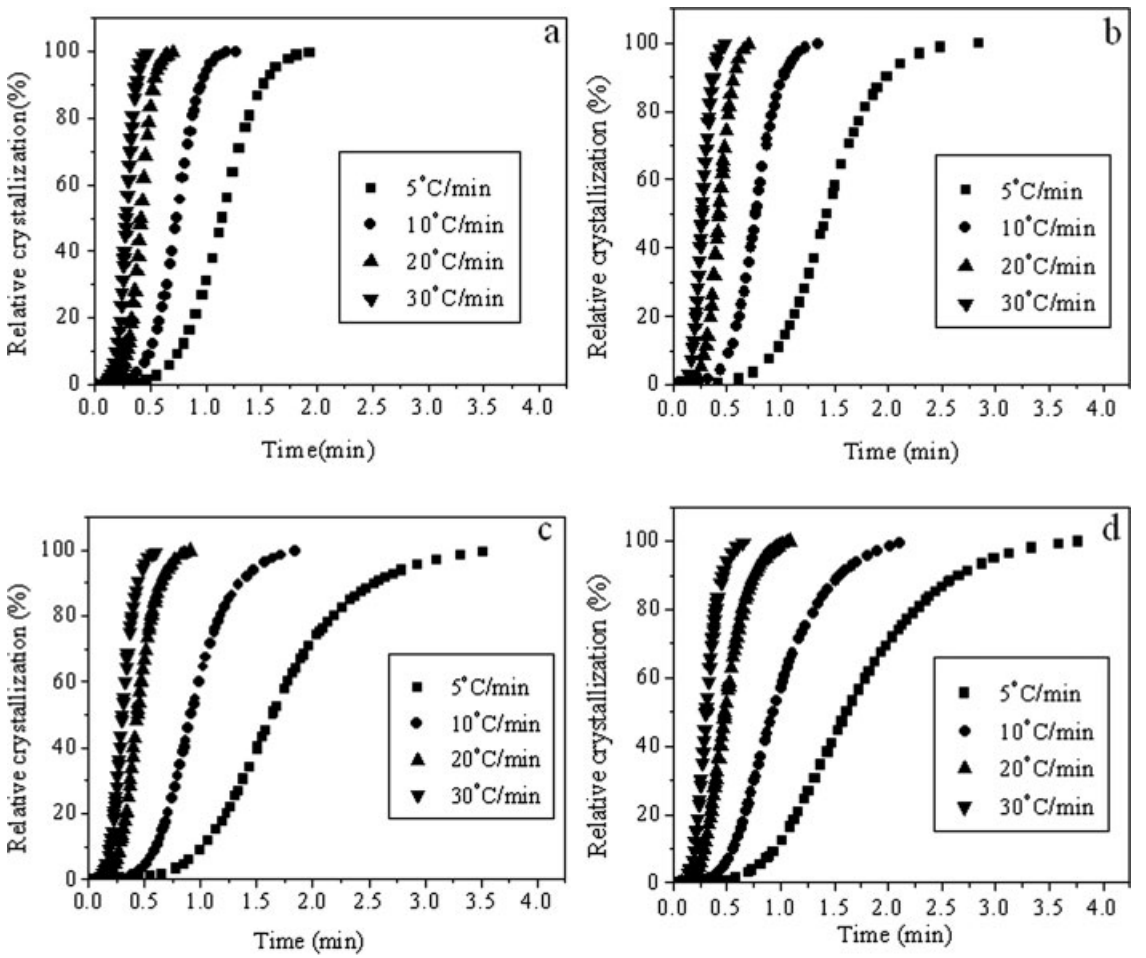

Figure 2 Development of the relative crystallinity with the crystallization time for (a) S40, (b) S50, (c) S80, and (d) S100.

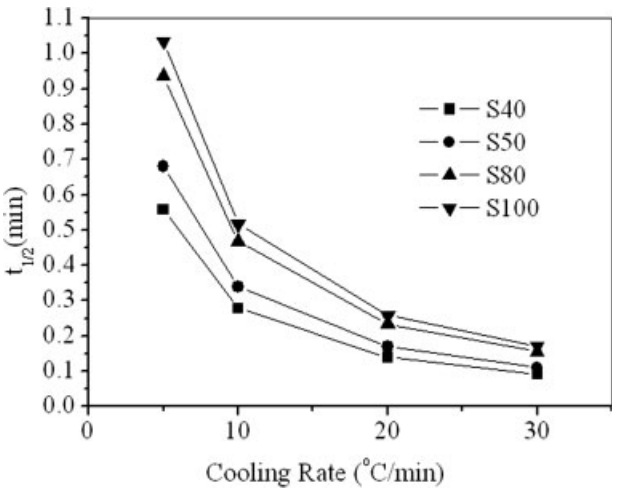

Figure 3 $t_{1/2}$ in the nonisothermal process at different cooling rates for the systems with different DBP ratios.

ratio in the diluent mixture increased. The overall crystallizing rate is controlled by two factors, namely, nucleation and growth. The increase of DBP in the diluent mixture increased the viscosity of the system and the interaction between PVDF and the diluent mixture; this not only prevented crystal nucleation but also lowered the transference ability of polymer segments. On the contrary, increasing the cooling rate could raise the nucleation ability and cause the reduction of $t_{1/2}$, as shown in Figure 3.

Ozawa analysis of nonisothermal crystallization

Ozawa[24] extended the Avrami equation to nonisothermal crystallization processes by assuming that a sample is cooled at a constant rate, and Evans[23] proved the application through mathematical analysis. However, there must be many restricting conditions in applications. For example, not only are the secondary crystallization and the dependence of the fold length on temperature ignored, but exponent m is assumed to be a constant independent of temperature. According to the Ozawa theory, $X(T)$ at temperature T and cooling rate Φ is given by

$$1 - X(T) = \exp[-k(T)/\Phi^m] \tag{3}$$

where $k(T)$ is the cooling function of nonisothermal crystallization at temperature T and m is the Ozawa exponent, depending on the nucleation mechanism and the growth dimension. Equation (3) can be rewritten as follows:

$$\log[-\ln(1 - X(T))] = \log k(T) - m \log \Phi \tag{4}$$

m and $\log k(T)$ can be easily determined from the slope and intercept on the basis of the linear relationship between $\log\{-\ln[1 - X(T)]\}$ and $\log \Phi$.

For all blends, Ozawa plots of $\log\{-\ln[1 - X(T)]\}$ against $\log \Phi$ are shown in Figure 4. Although the plots show some linearity, some curvature is also present. The change in the slope indicates that m is not constant with temperature, and cooling function $k(T)$ cannot be determined. The most likely reason for this may be the occurrence of secondary crystallization in the cooling process. The failure of the Ozawa model to describe the nonisothermal behavior of PVDF in the PVDF/DBP/DEHP blends probably lies in ignoring secondary crystallization and the variable value of the cooling function over the entire crystallization process.

Avrami analysis modified by Jeziorny

Avrami analysis modified by Jeziorny[25] has also been used to describe the nonisothermal crystallization kinetics of polymers. The dependence of the relative crystallinity as a function of crystallization time t $[X(t)]$ for nonisothermal crystallization processes is calculated with a modified Avrami equation shown as eq. (5) or eq. (6):

$$X(t) = 1 - \exp\left(-Z_t t^n\right) \tag{5}$$

$$\log[-\ln(1 - X(t))] = n \log t + \log Z_t \tag{6}$$

where n is the Avrami exponent, a mechanism constant depending on the nucleation type and growth process; Z_t is the Avrami rate constant, involving nucleation and growth parameters; and t is the crystallization time. Considering the process to be nonisothermal, Jeziorny suggested that rate parameter Z_t should be corrected by the influence of cooling rate Φ. The final form of the parameter characterizing the kinetics of nonisothermal crystallization (Z_c) is given as eq. (7):

$$\log Z_c = \frac{\log Z_t}{\Phi} \tag{7}$$

If eq. (6) adequately describes the nonisothermal crystallization behavior of a polymer, the straight-line relationship of $\log\{-\ln[1 - X(t)]\}$ versus $\log t$ would give the values of n and Z_t or Z_c from the slopes and intercepts, respectively. The Avrami plots of $\log\{-\ln[1 - X(t)]\}$ versus $\log t$ for PVDF/DBP/DEHP blends are shown in Figure 5. The initial and final relative degrees of crystallinity used in Figure 5 are approximately 2 and 99.6%. The linearity of the plots is poor, and each plot presents two obvious sections corresponding to the primary crystallization stage and the secondary crystallization stage. It is also clear that when the DBP ratio increases in the diluent mixture, the plots show a larger portion for the secondary crystallization stage. These results indicate that the

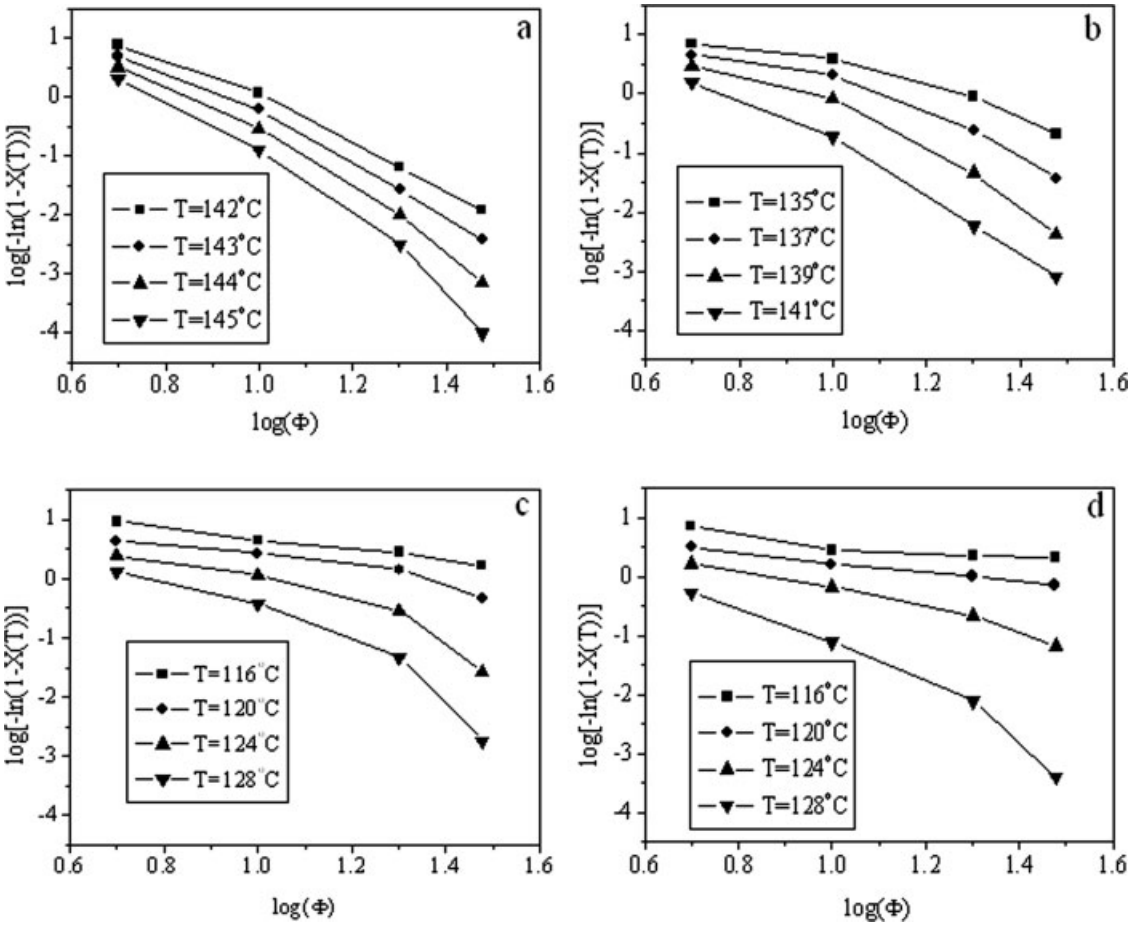

Figure 4 Ozawa plots for nonisothermal crystallization of (a) S40, (b) S50, (c) S80, and (d) S100.

secondary crystallization of PVDF existed in the process of nonisothermal crystallization and was enhanced by an increase of DBP in the diluent mixture.

The calculated values of n, Z_t, and Z_c are listed in Table IV. At the primary stage, Avrami exponent n_1 lies between 4 and 5. Linares and Acosta[26] reported that the values of n for PVDF ranged from 2.3 to 3.6 in the process of nonisothermal crystallization.[26] The larger values of n (>4) in this study implied a more complicated crystallization mechanism of PVDF in the diluent mixture, which is difficult to explain at present. The values of crystallization rate parameter Z_{c1} were comparable for every sample. At a specific cooling rate, the values of Z_{c1} for PVDF decreased with the DBP ratio in the diluent mixture increasing. DBP exhibited higher viscosity and stronger interaction with PVDF than DEHP, which brought resistance for the transport of the polymeric segments to the growing crystal surface and reduced the rate of crystal growth. At the same time, the values of Z_{c1} increased with the increase in the cooling rate. Increasing the cooling rate provided the system with more energy to improve the activity of chain segments, thus resulting in the increase in crystallization rate parameter Z_{c1}. At the secondary crystallization stage, Avrami exponent n_2 ranged from 2.1 to 4.3 and decreased with an increase in the DBP ratio in the diluent mixture. The smaller values of n implied that the crystallization mechanism became simpler. Especially for S100, n_2, ranging from 2.1 to 2.4, indicated that the form of spherulite growth transformed into two-dimensional or lamellar-like crystal growth.

Combined Ozawa–Avrami approach

By combining eqs. (4) and (6), Mo et al.[27] derived another kinetic equation for nonisothermal crystallization behavior to relate the crystallinity to cooling rate Φ and crystallization time t (or temperature T). The relation between Φ and t was defined for a given degree of crystallinity:

$$\log Z_t + n \log t = \log k(T) - m \log \Phi \tag{8}$$

or

$$\log \Phi = \log F(T) - b \log t \tag{9}$$

The parameter $F(T) = [k(T)/Z_t]^{1/m}$ is the value of the cooling rate, which has to be chosen at the unit of

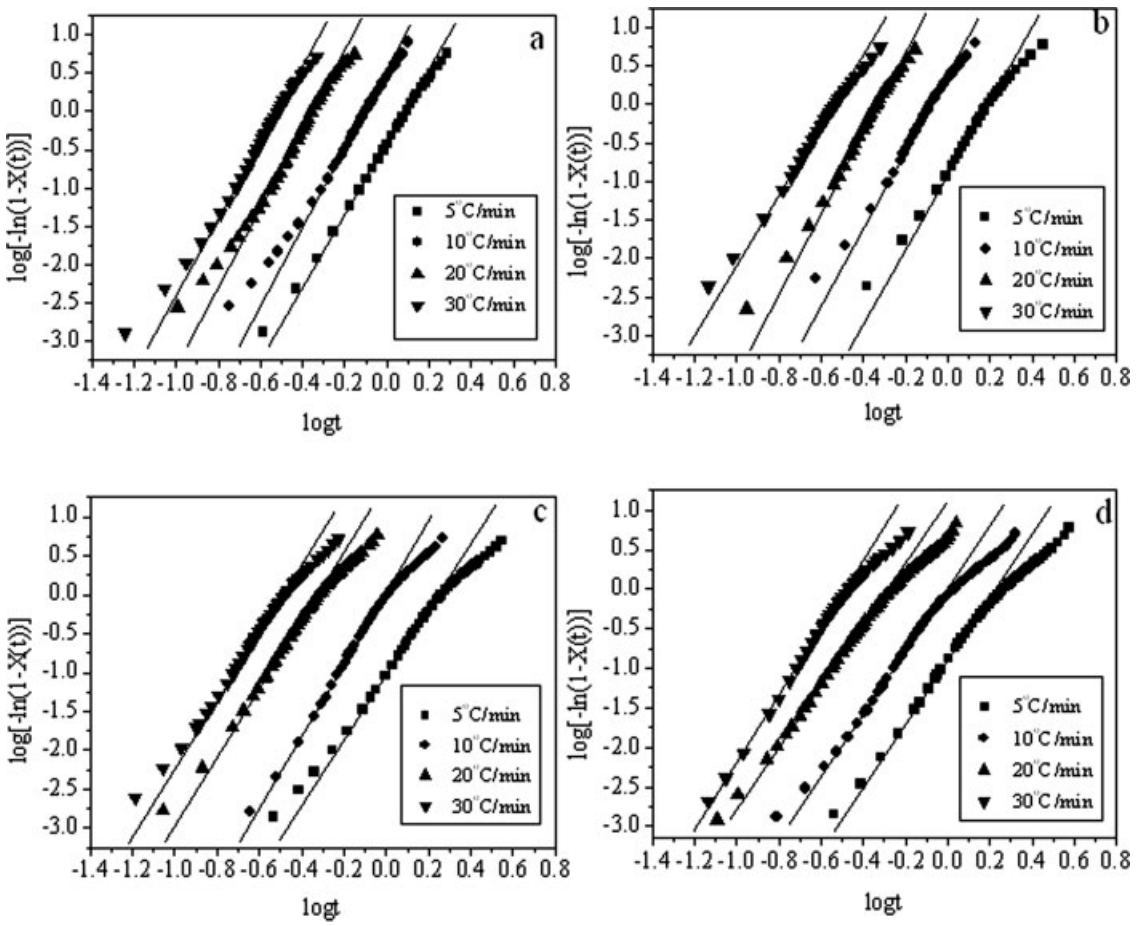

Figure 5 Plots of log $\{-\ln[1 - X(t)]\}$ versus log t for nonisothermal crystallization of (a) S40, (b) S50, (c) S80, and (d) S100.

crystallization time when the measured system amounts to a certain degree of crystallinity. The smaller the value of $F(T)$ is, the higher the crystallization rate becomes. Therefore, $F(T)$ has a definite physical and practical meaning. Parameter b is the ratio of the Avrami and Ozawa exponents; that is, $b = n/m$. From eq. (9), it follows that, at a given degree of crystallinity, the plot of log Φ versus log t should be a straight line with an intercept of log $F(T)$ and a slope of b. From the obtained plots for PVDF/DBP/DEHP blends given in Figure 6, it is clear that there is a good linear relationship between log Φ and log t for all plots.

Because the maximum of crystallization used in this study was 80%, the Mo approach just analyzed the kinetics of primary crystallization. The values of $F(T)$ and b for the blends are listed in Table V. The value of $F(T)$ increased with the crystallinity increasing and also with the DBP ratio in the diluent mixture increasing. In other words, the increase in the viscosity of the system and the interaction between PVDF and the diluent mixture could reduce the crystallizing rate, and this was consistent with those analyzed with the Avrami model modified by

TABLE IV
Kinetic Parameters for PVDF in PVDF/DBP/DEHP Blends from the Avrami Analysis

Sample	Cooling rate (°C/min)	Primary crystallization stage			Secondary crystallization stage		
		n_1	Z_{t1}	Z_{c1}	n_2	Z_{t2}	Z_{c2}
S40	5	4.8	0.398	0.832	3.9	0.449	0.852
	10	4.9	3.258	1.125	4.3	2.805	1.109
	20	5.0	53.951	1.221	2.9	15.849	1.148
	30	4.9	338.065	1.214	3.2	63.096	1.148
S50	5	4.9	0.130	0.665	2.8	0.331	0.802
	10	5.0	2.735	1.106	3.9	1.955	1.072
	20	5.0	52.240	1.219	3.6	18.408	1.157
	30	4.7	322.107	1.212	3.3	61.944	1.147
S80	5	4.4	0.112	0.646	2.2	0.306	0.789
	10	4.6	1.298	1.028	2.5	1.122	1.012
	20	4.3	25.883	1.177	2.5	6.998	1.102
	30	4.4	161.436	1.185	2.8	22.284	1.109
S100	5	4.0	0.109	0.642	2.1	0.288	0.780
	10	4.0	1.101	1.010	2.1	0.927	0.992
	20	4.0	13.709	1.140	2.2	4.198	1.074
	30	4.2	107.399	1.169	2.4	13.964	1.092

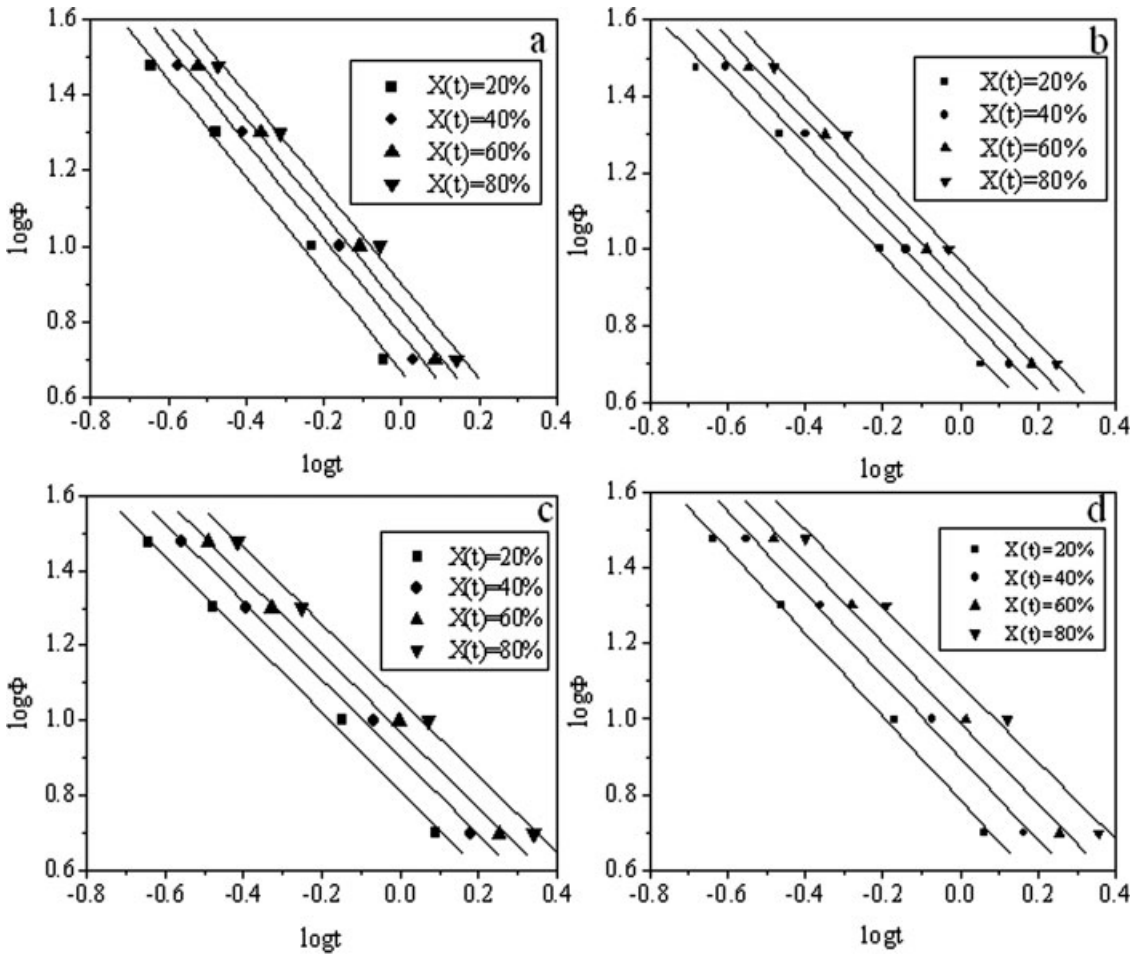

Figure 6 Log Φ versus log t for PVDF/DBP/DEHP blends from the combined Avrami and Ozawa equation for (a) S40, (b) S50, (c) S80, and (d) S100.

Jeziorny. The value of b ranged from 1.29 to 1.02 and changed little for the same sample with different crystallinity. The combined Avrami–Ozawa equation satisfactorily described the primary crystallization behavior of PVDF in the diluent mixture.

Crystallization activation energy (ΔE)

From the variation of T_p found in differential thermal analysis with the cooling rate, Kissinger[28] derived ΔE for the transport of the polymeric segments to a growing crystal surface as the form shown in eq. (10):

TABLE V
Values of b and $F(t)$ at Various Values of $X(t)$ for PVDF in PVDF/DBP/DEHP Blends

$X(t)$ (%)		20	40	60	80
S40	b	1.29	1.27	1.26	1.26
	$F(t)$	4.656	5.834	6.792	7.943
S50	b	1.08	1.08	1.08	1.08
	$F(t)$	5.875	7.031	8.017	9.333
S80	b	1.04	1.04	1.03	1.02
	$F(t)$	6.501	7.962	9.376	11.324
S100	b	1.10	1.08	1.06	1.02
	$F(t)$	6.557	8.145	9.75	12.30

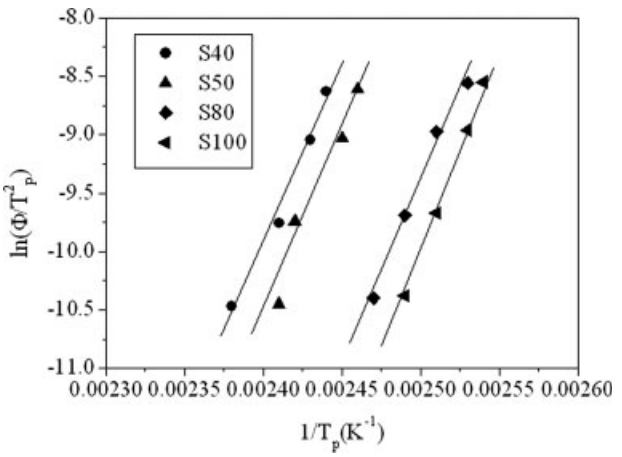

Figure 7 Kissinger plots for PVDF in PVDF/DBP/DEHP blends.

TABLE VI
ΔE Values for PVDF in PVDF/DBP/DEHP Blends

Sample	ΔE (kJ mol^{-1} k^{-1})
S40	−253.9
S50	−264.3
S80	−297.5
S100	−316.0

$$\frac{d[\ln(\Phi/T_p^2)]}{d(1/T_p)} = \frac{-\Delta E}{R} \tag{10}$$

The parameters have the same meaning as indicated in the previous test. ΔE could be calculated from the slopes of plots of $\ln(\Phi/T_p^2)$ versus $1/T_p$, as shown in Figure 7. As shown in Figure 7, the plots of $\ln(\Phi/T_p^2)$ versus $1/T_p$ for all samples presented a good linear relationship. The values of ΔE for PVDF in the diluent mixture, as calculated from the slope of the corresponding curves, are listed in Table VI. A decreasing value of ΔE with an increasing DBP ratio in the mixed diluent indicated that increasing the viscosity of the system and the interaction between the diluent and PVDF caused the decrease in the activation energy.

CONCLUSIONS

With the DSC data obtained at various cooling rates, the Ozawa, modified Avrami, and Mo approaches were used for the investigation of the nonisothermal crystallization kinetics of PVDF in PVDF/DBP/DEHP blends via only S–L phase separation. DSC exotherms of nonisothermal crystallization showed that all the crystallization parameters of PVDF (T_o, T_e, and T_p) decreased with the DBP ratio in the diluent mixture increasing. On the other hand, $t_{1/2}$ increased as the DBP ratio in the diluent mixture increased or the cooling rate decreased.

The Ozawa model failed to describe the nonisothermal behavior of PVDF in PVDF/DBP/DEHP blends, probably because of the negligence of secondary crystallization. The Avrami equation modified by Jeziorny was successful in describing the nonisothermal crystallization process of PVDF. It was found that secondary crystallization existed in the process of nonisothermal crystallization and was enhanced by the DBP ratio in the diluent mixture increasing. Avrami exponent n_2 at the secondary crystallization stage became smaller (2.1–2.4) when the DBP ratio was higher in the diluent mixture, and this implied that the crystallization mechanism became simpler and the form of spherulite growth transformed into two-dimensional or lamellar-like crystal growth. The kinetics of primary crystallization could be analyzed by not only the modified Avrami equation but also the Mo approach. The analysis of these two methods indicated that the crystallization rate increased with the DBP ratio in the diluent mixture decreasing or the cooling rate increasing. ΔE of PVDF was calculated with the Kissinger theory and indicated that increasing the DBP ratio in the diluent mixture caused the decrease in the activation energy.

References

1. Jiang, Z.; Carroll, B.; Abraham, K. M. Electrochim Acta 1997, 42, 2667.
2. Periasamy, P.; Tatsumi, K.; Shikano, M.; Fujieda, T.; Sakai, T.; Saito, Y.; Mizuhata, M.; Kajinami, A.; Deki, S. Solid State Ionics 1999, 126, 285.
3. Tarascon, J. M.; Gozdz, A. S.; Schmutz, C.; Shokoohi, F.; Warren, P. C. Solid State Ionics 1996, 86, 49.
4. Gozdz, A. S.; Schmutz, C. N.; Tarascon, J. M.; Warren, P. C. U.S. Pat. 5,540,741 (1997).
5. Boudin, F.; Andrieu, X.; Jehoulet, C.; Olsen, I. I. J Power Sources 1999, 81, 804.
6. Kataoka, H.; Saito, Y.; Sakai, T. J Phys Chem B 2000, 104, 11460.
7. Michot, T.; Nishimoto, A.; Watanabe, M. Electrochim Acta 2000, 45, 1347.
8. Magistris, A.; Mustarelli, P.; Parazzoli, F.; Quartarone, E.; Paiggio, P.; Bottino, A. J Power Sources 2001, 97, 657.
9. Hiatt, W. C.; Vitzthum, G. H.; Wagener, K. B.; Gerlach, K.; Josefiak, C. ACS Symp Ser 1985, 269, 229.
10. Smith, S. D.; Shipman, G. H.; Floyd, R. M.; Freemyer, H. T.; Hamrock, S. J.; Yandrasits, M. A.; Walton, G. S. U. S. Pat. 0,058,821 (2005).
11. Gu, M.; Zhang, J.; Wang, X.; Tao, H.; Ge, L. Desalination 2006, 192, 160.
12. Lloyd, D. R.; Kim, S. S.; Kinzer, K. E. J Membr Sci 1990, 52, 239.
13. Matsuyama, H.; Okafuji, H.; Maki, T.; Teramoto, M.; Kubota, N. J Membr Sci 2003, 233, 199.
14. Zhang, C.-F.; Zhu, B.-K.; Ji, G.-L.; Xu, Y.-Y. J Appl Polym Sci 2006, 99, 2782.
15. Marand, H.; Alizadeh, A.; Farmer, R.; Desai, R.; Velikov, V. Macromolecules 2000, 33, 3392.
16. Alizadeh, A.; Sohn, S.; Quinn, J.; Shank, L. C.; Derrell Iler, H. Macromolecules 2001, 34, 4066.
17. Marand, H.; Alizadeh, A.; Sohn, S.; Xu, J.; Farmer, R.; Prabhu, V.; Cronin, S.; Velikov, V. Annu Tech Conf 2001, 2, 1856.
18. Neidhöfer, M.; Beaume, F.; Ibos, L.; Bernès, A.; Lacabanne, C. Polymer 2004, 45, 1679.
19. Lim, G. B. A.; Lloyd, D. R. Polym Eng Sci 1993, 33, 529.
20. Lim, G. B. A.; McGuire, K. S.; Lloyd, D. R. Polym Eng Sci 1993, 33, 537.
21. Liu, B.; Du, Q.; Yang, Y. J Membr Sci 2000, 180, 81.
22. Brandrup, J.; Immergut, E. H.; Grulke, E. A. Polymer Handbook, 4th ed.; Wiley: New York, 1999.
23. Evans, U. R. Trans Faraday Soc 1945, 11, 365.
24. Ozawa, T. Polymer 1971, 12, 150.
25. Jeziorny, A. Polymer 1978, 19, 1142.
26. Linares, A.; Acosta, J. L. Polymer 1997, 38, 2741.
27. Liu, T.; Mo, Z.; Wang, S.; Zhang, H. Polym Eng Sci 1997, 37, 568.
28. Kissinger, H. E. J Res Natl Bur Stand 1956, 57, 217.